BIOCHEMISTRY
including biophysical chemistry & molecular biology

Article

pubs.acs.org/biochemistry

Mass Spectrometric Determination of Disulfide Bonds in the Biologically Active Recombinant HBx Protein of Hepatitis B Virus

Kaveri Sidhu,[†] Saravanan Kumar,[‡] Vanga Siva Reddy,[‡] and Vijay Kumar*,[†]

[†]Virology Group and [‡]Plant Transformation Group, International Center for Genetic Engineering and Biotechnology, Aruna Asaf Ali Marg, New Delhi 110067, India

Supporting Information

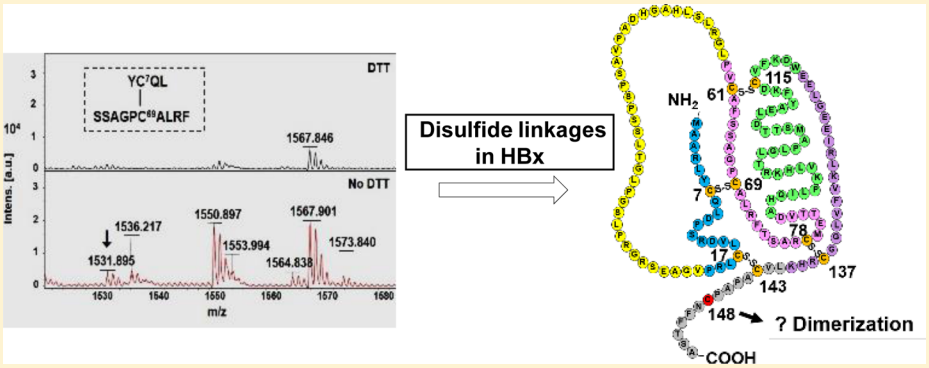

ABSTRACT: Many proteins rely on disulfide bonds formed between pairs of cysteines for the stability of their folded state and to keep regulatory control over their functions. The hepatitis B virus-encoded HBx oncoprotein is known to perform an overwhelming array of functions in the cell and has been implicated in the development of hepatocellular carcinoma. However, its structure has not been elucidated. HBx carries nine conserved cysteine residues that have proven to be crucial for its various functions. However, the status of disulfide bonds between the cysteine residues reported in previous studies remains discrepant because of the use of refolded recombinant HBx that may contain non-native disulfides. Now we have determined the disulfide linkages in soluble and biologically active recombinant maltose binding protein−HBx fusion protein using matrix-assisted laser desorption ionization time-of-flight mass spectrometry. We report four disulfide linkages in HBx protein, viz., between Cys^{7} and Cys^{69}, Cys^{61} and Cys^{115}, Cys^{78} and Cys^{137}, and Cys^{17} and Cys^{143}, based on the differential mobility of corresponding disulfide-linked peptide ions under reducing and nonreducing conditions. Cys^{148} was observed to be free. Site-directed mutagenesis of Cys^{143} and Cys^{148} with serine and functional analyses of these mutants affirmed the importance of these residues in the ability of HBx to potentiate Cdk2/cyclin E kinase activity and transcriptionally activate promoter reporter gene activity. Thus, this study identifies native disulfide linkages in the structure of a biologically active viral oncoprotein.

Tumor viruses are well-known to encode oncoproteins that have honed multitasking abilities, including taking over the host cellular machinery. These viral oncoproteins share some common features such as their small size, intrinsically disordered structure, and dimerization potential, which allow them to conduct their myriad of functions. While intrinsic disorder allows flexibility in the protein structure to interact with multiple partners and play diverse roles, it also hinders their structural determination. Not surprisingly, 79% of the cancer-associated proteins, including c-Myc, p53, CREB, and viral oncoproteins E6, E7, and HBx, embody predicted regions of disorder of varying lengths.[1]

The HBx oncoprotein of hepatitis B virus is associated with the development of hepatocellular carcinoma.[2,3] One of the well-recognized functions of HBx protein is its ability to transactivate several viral and host gene promoters to sustain the oncogenic program (reviewed in ref 4). Even as HBx does not bind directly to DNA, it can alter the DNA binding characteristics of many transcription factors.[4,5] In addition, HBx initiates cell transformation by modulating various host cell processes such as cell cycle, DNA damage response, and signal transduction pathways, among many others.[6−10] HBx is a relatively small polypeptide (154 amino acids) having a modular organization of its functional domains (A−F) that exhibit functions like transactivation, transrepression, cell signaling, etc.[4,11−14] Like many other transcription factors, HBx is also known to form both homo- and heterodimers.[15,16] These dimers are sensitive to reducing agents and, therefore, can be attributed to disulfide linkages.[17] Considering that HBx carries nine conserved cysteine residues,[18] it suggests the possibility of up to four disulfide linkages and at least one free cysteine residue presumably involved in dimerization function.

Received: February 1, 2014
Revised: June 24, 2014
Published: June 27, 2014

   dx.doi.org/10.1021/bi500140t | *Biochemistry* 2014, 53, 4685−4695

The importance of conserved cysteine residues in HBx activity has been functionally characterized by site-directed mutagenesis. For example, Cys^{115} of HBx has been found to be crucial for mitochondrial targeting, and mutation of Cys^{137} results in a failure to activate the STAT3 pathway.[19,20] Cys^{61} and Cys^{69} mutations are critical for the transactivation function of HBx,[11] while HBx mutated at Cys^{69} alone is sufficient to inhibit the binding of HBx to damage-specific DNA binding protein 1 (DDB1) that causes inhibition of DNA repair.[21] Further, a mutant HBx with all cysteine residues mutated to serine fails to bind UVDDB.[22] Thus, the conserved cysteines seem to impart a critical role in HBx functioning. Thus, a crucial step in understanding the structure of HBx is to discern the role of the conserved cysteine residues.

Despite a wealth of information about diverse functions associated with HBx, we have rather limited information about the HBx structure. All attempts in the past to solve this problem as well as the crystal structure of HBx have eluded many scientific groups so far, and this has been attributed to its disordered structure. There are just a few reports, albeit contradictory, assigning the disulfide linkages in HBx.[16,23,24] Besides, the absence of any structural homology partner has been an impediment in the smooth progress of this field. In this study, we expressed and purified the MBP-tagged HBx protein in a soluble form. We show that the MBP−HBx fusion protein exhibits the transactivation and Cdk2/cyclin E kinase activity potentiation function like native HBx. Further, we have assigned four disulfide linkages in HBx protein with the help of MALDI-TOF/TOF mass spectrometry analysis and corroborated these findings with new mutational studies.

EXPERIMENTAL PROCEDURES

Buffers and Chemicals. Unless otherwise mentioned, all buffers and chemicals were from Sigma-Aldrich (St. Louis, MO). All restriction enzymes were from Fermentas (Waltham, MA), and Taq DNA polymerase and DNA ligase were procured from Intron Biotechnology (Kyungki-Do, South Korea). Amylose resin beads used for affinity purification were procured from New England Biolabs (Ipswich, MA). Trypsin and chymotrypsin were mass spectrometry grade and from Promega (Madison, WI). Recombinant CDK2/CCNE1 protein (Abcam, Cambridge, MA) and histone H1 (Roche) were used for *in vitro* phosphorylation assays. [γ-^{32}P]ATP and [^{14}C]chloramphenicol were from PerkinElmer (Waltham, MA). The polyclonal Cdk 2 antibody and monoclonal HBx antibody were from Santa Cruz Biotechnology (Santa Cruz, CA). Silica gel thin layer chromatography plates were from E. Merck.

Development of HBx Recombinants. The development of the eukaryotic expression vector for the wild-type HBx gene (X0) (GenBank accession number X00715) and its mutants [X1 (Cys^{7} to Thr), X2 (Cys^{61} to Thr), X3 (Cys^{69} to Thr), X4 (Cys^{137} to Thr), X14 (Δ141−154), and X15 (Δ1−57,Δ141−154)] has been described previously.[25] The mutants of HBx [X143 (Cys^{143} to Ser) and X148 (Cys^{148} to Ser)] were generated by site-directed mutagenesis using the X0 template, common forward primer F (5′-CGGAATTCATGGCTGCTAGGCTGT), and specific reverse primers R143 (5′-ATTGACTCGAGTTAGG-CAGAGGTGAAAAAGTTGCATGGTGCTGGTGC**GCT**GA-CCAATTTGTG) and R148 (5′-ATTGACTCGAGTTAGGC-AGAGGTGAAAAAGTT**GCT**TGGTGCTGGTGC) for X143 and X148, respectively. The polymerase chain reaction-amplified fragments were cloned into the pSGI vector[26] (X143 and X148) between the EcoRI and XhoI sites. The mutations were confirmed by DNA sequencing.

The pMAL_TEV vector was derived from pMAL-p2X (New England Biolabs) by replacing the factor Xa protease cleavage site with that of the tobacco etch virus protease cleavage site. The factor Xa cleavage site from the pMAL-p2X vector was restricted out using SacI and BamHI restriction enzymes and replaced by the following pair of oligonucleotides having a TEV recognition sequence: TEV Forward (5′-CTAACAACAACAACAACAAC-AACAACAACAACCTGGGCGAAAACCTGTATTTTCAG-GGTGAATTCCTCGAGG-3′) and TEV Reverse (5′-GATC-CCTCGAGGAATTCACCCTGAAAATACAGGTTTTCGC-CCAGGTTGTTGTTGTTGTTGTTGTTGTTGTTAG-AGCT-3′). Oligos were annealed to form SacI and BamHI adaptor ends and ligated into the pMAl-p2X vector. MBP−X0 fusion recombinant was developed by cloning a 465 bp EcoRI fragment of X0 from the pSG5 vector[11] into the pMAL_TEV vector. Similarly, the MBP−X143 and MBP−X148 fusion recombinants were developed by cloning X143 and X148 mutants as EcoRI/XhoI fragments into the pMAL_TEV vector. RSV_CAT and Jun_CAT promoter reporter constructs have been described previously.[12]

Expression and Purification of MBP−HBx Fusion Proteins. The MBP−HBx fusion genes (MBP−X0, MBP−X143, and MBP−X148) were transformed into the SHuffle strain of *Escherichia coli*.[27] This strain harbors *trxB gor* suppressor mutations, which diminishes the reducing potential of its cytoplasm, and has a copy of disulfide bond isomerase *DsbC* that allows disulfide bond formation in the cytoplasm. Cells were grown in 1 L of LB containing 100 μg/mL ampicillin at 37 °C until it reached an optical density of 0.6. The culture was induced with 0.5 mM isopropyl β-D-1-thiogalactopyranoside for 16−18 h at 37 °C and harvested. The cells were washed once with PBS and lysed in buffer [50 mM Tris-HCl (pH 7.5), 150 mM NaCl, 1 mM EDTA, 1 mM DTT, 1 mM PMSF, protease inhibitor cocktail (Roche), and 20 mg/mL lysozyme] at 4 °C for 1 h while being shaken followed by sonication (Sonics, Milpitas, CA) for 1 h at 30% amplitude (10 s pulse on, 10 s pulse off) at 4 °C. The lysed cells were centrifuged at 15000*g* for 1 h at 4 °C, and the supernatant was incubated overnight at 4 °C with 1 mL of amylose resin beads equilibrated with 10 bed volumes of binding buffer [50 mM Tris-HCl (pH 7.5), 150 mM NaCl, and 1 mM EDTA]. The beads were washed with 5 volumes of binding buffer and finally eluted in 3 volumes of elution buffer [50 mM Tris-HCl (pH 7.5), 150 mM NaCl, 1 mM EDTA, 1 mM DTT, and 10 mM maltose]. DTT (1 mM) was added to keep the free cysteine(s) in a reduced state without affecting the integrity of natively formed disulfide bonds as reported previously.[28] The purity of the eluted protein was checked by 10% sodium dodecyl sulfate−polyacrylamide gel electrophoresis (SDS−PAGE) followed either by Coomassie staining or by Western blotting with the anti-HBx antibody. Aliquots of purified protein samples were frozen in liquid nitrogen and stored at −80 °C until further use.

Untagged wild-type full length HBx expression vector pET-3d was transformed in *E. coli* BL21-DE3 cells, and the protein was purified from inclusion bodies and refolded as described previously.[29]

Reduction, Alkylation, and Proteolytic Digestion of MBP−HBx Fusion Proteins. The purified MBP−HBx proteins were dialyzed against 20 mM NH_4HCO_3 and concentrated to 1 mg/mL using a Vivaspin centrifugal concentrator (30000 kDa cutoff) (Sartorius, Goettingen, Germany). Aliquots (10 μg) of MBP−X0, MBP−X143, and MBP−X148 fusion proteins were

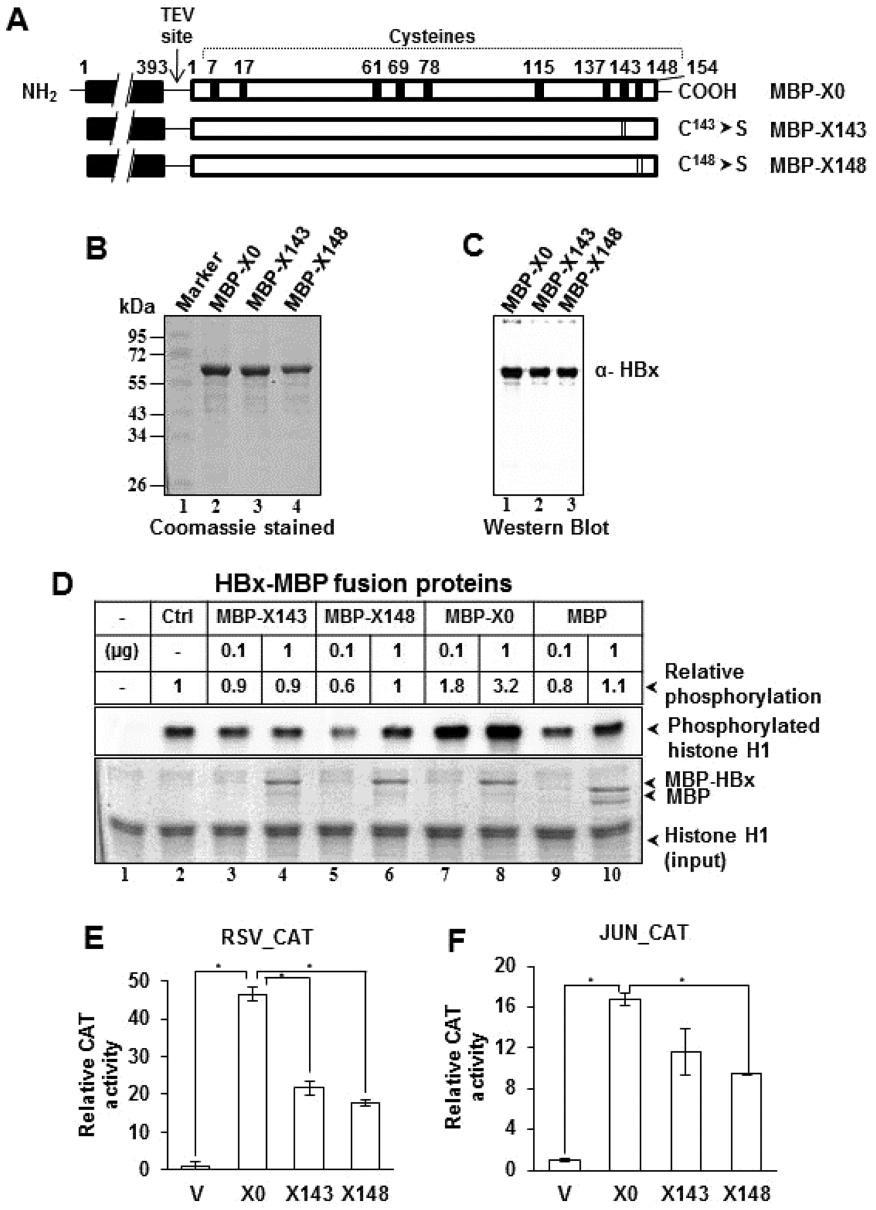

Figure 1. Schematic representation of the MBP−HBx fusion proteins. (A) The MBP region (393 amino acids) is localized at the N-terminus of MBP−HBx fusion proteins (shown as a black bar). The HBx recombinants (X0, X143, and X148) were cloned at the C-terminus of MBP (shown as a white bar). Wild-type HBx (X0) is 154 amino acids in length, showing its nine conserved cysteines at positions 7, 17, 61, 69, 78, 115, 137, 143, and 148 (top). The two cysteine mutants of HBx (X143 and X148) are shown below. (B and C) Affinity-purified MBP−X0, MBP−X143, and MBP−X148 fusion proteins were subjected to reducing SDS−PAGE followed by (B) Coomassie staining and (C) Western blotting using the anti-HBx monoclonal antibody. (D) Phosphorylation of histone H1 in the presence of 0.1 and 1 μg of affinity-purified MBP−X143, MBP−X148, MBP−X0, and MBP recombinant proteins (top). The Coomassie-stained gel of the phosphorylation reaction mixture is shown below as a loading control. (E and F) HEK293 cells were transfected with 1 μg of vector DNA (V) or expression plasmids for HBx recombinants (X0, X143, and X148) along with the (E) RSV_CAT (1 μg) or (F) JUN_CAT (1 μg) reporter plasmid, and the resultant chloramphenicol acetyltransferase activity was determined. Results are shown as means of three independent observations ± the standard deviation. Statistical significance was tested at a $p < 0.01$ probability level vs the vector or wild type.

subjected to denaturation, reduction, and alkylation followed by their proteolytic digestion with either trypsin or chymotrypsin for different periods of time (Figure S1 of the Supporting Information). Briefly, the protein was denatured by addition of SDS to a final concentration of 0.2% and then heated at 95 °C for 5 min. Following denaturation, protein samples were reduced in the presence of 10 mM DTT at 56 °C for 45 min under a N_2 atmosphere. The reduced protein sample was alkylated in the dark by addition of 50 mM iodoacetamide at 25 °C for 30 min. The samples were diluted to 2 mM DTT using 10 mM NH_4HCO_3 and 1 mM $CaCl_2$ and digested with trypsin or chymotrypsin (1:20 enzyme:protein ratio) for 5, 10, or 20 min or overnight at 37 °C. The reaction was stopped by addition of 0.1% trifluoroacetic acid, and the samples were desalted using C18 micro spin columns (Sartorius), vacuum-dried, and stored at −20 °C until further use. The tryptic and chymotryptic peptides were analyzed by MALDI-TOF/TOF mass spectrometry and liquid chromatography and tandem mass spectrometry (LC−MS/MS) as described in the Supporting Information.

dx.doi.org/10.1021/bi500140t | *Biochemistry* 2014, 53, 4685−4695

***In Vitro* Kinase Assay.** Purified recombinant MBP, MBP−X0, MBP−X143, and MBP−X148 fusion proteins (0.1 or 1 μg) were used in the protein kinase reaction mixture comprising 0.1 μg of recombinant Cdk2/cyclin E, 2 μg of substrate histone H1 (Roche), and [γ-^{32}P]ATP (3000 Ci/mmol) in kinase buffer [50 mM Tris-HCl (pH 7.5), 10 mM $MgCl_2$, 1 mM DTT, 2.5 mM sodium pyrophosphate, 1 mM β-glycerophosphate, and 1 mM sodium orthovanadate]. The reaction mixture was incubated at 30 °C for 30 min and the reaction stopped by adding an equal volume of Laemmli buffer and heating for 5 min followed by electrophoresis in a 12% SDS−polyacrylamide gel. After being dried, the gel was exposed to a phosphorimager (GE Healthcare Lifesciences, Piscataway, NJ) overnight and scanned on Typhoon scanner (GE Healthcare Lifesciences), and the intensities of bands were analyzed densitometrically.

In vitro phosphorylation studies were also performed using Cdk2 immunoprecipitates (IP) from the HBx-transfected cells. Human embryonic kidney HEK293 cells were transfected with expression plasmids with either full length HBx (X0) or its mutants (X143, X148, X1, X2, X3, X4, X14, or X15). Cells were harvested after 48 h and lysed in IP buffer [20 mM Tris-HCl (pH 7.5), 150 mM NaCl, 1 mM EDTA, 1 mM EGTA, 1% Triton X-100, 2.5 mM sodium pyrophosphate, 1 mM β-glycerophosphate, and 1 mM sodium orthovanadate] for 2 h at 4 °C. The cell extracts (1 mg of protein each) were incubated overnight with the anti-Cdk2 antibody (1 μg) followed by incubation with protein A agarose beads for 2 h at 4 °C as described previously.[7] The protein A bead-bound immune complexes were washed thrice with 1× PBS followed by two washes with kinase buffer. The Cdk2-immobilized protein A beads were incubated with substrate histone H1 (2 μg) and [γ-^{32}P]ATP in kinase buffer, and the reaction was conducted as detailed above.

Chloramphenicol Acetyltransferase (CAT) Assay. Transactivation activities of HBx and its mutants were analyzed by a CAT assay. The human hepatoma Huh7 cells were cotransfected with the pSG5, X0, X143, or X148 expression vector (1 μg each), along with RSV_CAT (1 μg) or JUN_CAT (1 μg) reporter plasmids using Lipofectamine 2000 (Invitrogen) following the manufacturer's instructions. Cells were harvested 48 h post-transfection, washed twice with 1× PBS, and lysed in IP buffer. The CAT assay was performed using 10 μg of protein from cell extract. The endogenous deacetylase activity was inactivated by incubation at 65 °C for 15 min followed by addition of the reaction mixture containing 1 μCi of [^{14}C]-chloramphenicol (50 Ci/mmol) and 0.5 mM acetyl-coenzyme A. The samples were incubated at 37 °C for 20 min as described previously.[11] The reaction was stopped by adding 1 mL of ethyl acetate, and the organic phase was separated and vacuum-dried. After being resuspended in 20 μL of ethyl acetate, the samples were spotted on a silica gel TLC plate and resolved using a chloroform/methanol (95:5) solvent mixture. The TLC plate was autoradiographed, and spots corresponding to the acetylated forms of chloramphenicol were quantified by densitometry and analyzed.

Bioinformatic Analysis. Disulfide linkages were predicted using an artificial neural network and web server DiANNA[30] (http://clavius.bc.edu/~clotelab/DiANNA/n).

RESULTS

Expression and Purification of Maltose Binding Protein (MBP)-Tagged Native and Mutant HBx. To determine the disulfide linkages formed in HBx protein due to the presence of nine conserved cysteines (Figure 1A), we first developed MBP−HBx fusion recombinants. The MBP tag is known to help maintain the fusion proteins in a soluble state in *E. coli*[31] and facilitate their translocation to the periplasmic compartment of *E. coli* where the redox potential is favorable for disulfide bond formation with the help of Dsb enzymes.[32] Besides, MBP does not have a cysteine residue in its primary sequence. We accomplished high-level expression of the MBP−HBx recombinants using the SHuffle strain of *E. coli*, most of which was apparently transported into the periplasmic space (Figure S2 of the Supporting Information). The MBP−X0 recombinant protein was affinity purified using amylose resin with a yield of ∼10 mg/L of bacterial culture with a purity of >98% (Figure 1B). Likewise, the HBx mutants MBP−X143 (Cys^{143} to Ser) and MBP−X148 (Cys^{148} to Ser) yielded ∼3 and ∼2.5 mg of fusion protein/L of culture, respectively (Figure 1B). The antigenicity of MBP−X0, MBP−X143, and MBP−X148 fusion proteins was confirmed by Western blotting using the anti-HBx antibody (Figure 1C).

Purified recombinant MBP−HBx, MBP−X143, and MBP−X148 proteins were analyzed by circular dichroism (CD) spectroscopy to study their secondary structure. The MBP tag alone showed a positive peak at 192 nm and two negative troughs at 200 and 222 nm that revealed a predominantly α-helical structure with random coils and some β sheet (Figure S3A of the Supporting Information). The positive peak in the MBP−HBx protein shifted between 195 and 200 nm with a negative shoulder at 225 nm, suggesting a shift from an α-helical structure in MBP to a β-strand along with disordered structure in the MBP−HBx protein. The MBP−X143 and MBP−X148 mutants exhibited altered structure with an α-helical content higher than that of the MBP−HBx protein (Figure S3A of the Supporting Information). Interestingly, in the presence of maltose (20 μM), all the recombinant proteins acquired more α-helical content, which is evident from the lower ellipticities for the two negative troughs at 210 and 222 nm (Figure S3B,C of the Supporting Information). It has been reported that MBP upon binding to oligosaccharides switches from an "open" conformation to a more "closed" conformation.[33] The closed form of MBP revealed the more subtle differences in the MBP−HBx protein and its MBP−X143 and MBP−X148 mutants (Figure S3B,C of the Supporting Information). The considerably lower negative troughs at 210 and 222 nm for the MBP−HBx protein compared to those of MBP suggest that HBx possesses some α-helix that contributes to the increased helical content of the MBP−HBx fusion protein (Figure S3B of the Supporting Information). However, the MBP−X143 and MBP−X148 mutants showed weaker negative peaks than the MBP−HBx fusion protein (Figure S3C of the Supporting Information). Apparently, the MBP−X143 and MBP−X148 mutants acquired structures somewhat altered compared to that of the MBP−HBx protein in the presence of maltose.

We next subtracted the molar ellipticity values of MBP from those of the MBP−HBx protein to obtain a CD spectrum representative of just HBx protein (HBx* in Figure S3B,D of the Supporting Information). The CD spectra thus obtained for HBx protein suggested α-helical content as evident by the two negative 210 and 222 nm troughs, albeit they were lower than those of MBP or MBP−HBx fusion protein. Also, the negative band between 195 and 200 nm suggests disorder in the HBx structure.

The C-Terminal Cysteines of HBx Are Essential for Its Activity. Of the nine conserved cysteine residues present in HBx, the two C-terminal cysteines (Cys^{143} and Cys^{148}) have been

Table 1. Masses of Disulfide-Linked Peptides Generated from Reduced, Alkylated, and Digested Samples of MBP−X0, MBP−X143, and MBP−X148 Fusion Proteins[a]

peptide sequence	theoretical m/z		experimental m/z	
	with DTT	without DTT	with DTT	without DTT
YC[7]QL-SSAGPC[69]ALRF	583.254, 1065.515	1531.703	not detected, 1065.4670	1531.895
LC[17]LRPV-VC[143]APAPC[148]NFF	757.439, 1182.507	1764.851	1567.7678,[b]not detected	1764.962
RGLPVC[61]AF-FKDC[115]VF	919.482, 815.367	1617.792	1119.5405,[c]not detected	1617.854
TSARC[78]M-GGC[137]RHKLV	741.302, 926.499	1550.735	not detected, 1039.619[d]	1550.897
FTSARC[78]METTVDAHQILPKVLKHK-VFVLGGC[137]R	2809.473, 907.482	3628.903	1641.763,[e]907.460	3628.821

[a]Cysteines under reducing conditions (with DTT) are carbamidomethylated, and methionines are oxidized. [b]L.C[17]LRPVGAESRGRPL.S. [c]L.SLRGLPVC[61]AF.S. [d]F.VLGGC[137]RHKL.V. [e]R.C[78]METTVNAHQILPK.V.

overlooked for their role in the biological activity of HBx. The two cysteines were mutated independently (Figure 1A), and their biological activities on potentiation of kinase activity of the Cdk2/cyclin E complex and transcriptional activation of promoters have been studied.[7,12]

HBx has been shown to enhance the phosphorylation potential of the Cdk2/cyclin E complex toward its substrates histone H1 and Rb.[7] Therefore, to assess the phosphorylation potential of the cysteine mutants of HBx, we conducted *in vitro* phosphorylation of histone H1 by the recombinant Cdk2/cyclin E complex in the presence of purified MBP−X0, MBP−X143, MBP−X148, and MBP recombinant proteins. As shown in Figure 1D, histone H1 phosphorylation was enhanced by nearly 3.2-fold in the presence of the MBP−X0 protein, indicating that the recombinant MBP−X0 protein was functional. Under similar conditions, the cysteine mutants of HBx, viz., MBP−X143 and MBP−X148, and MBP alone failed to stimulate *in vitro* phosphorylation, suggesting no role for MBP and the importance of cysteines of HBx in stimulating cdk2 activity. Upon comparison of the biological activity of MBP-tagged HBx with an untagged HBx protein, the MBP−HBx protein exhibited Cdk2/cyclin E kinase activity higher (3.5-fold) than that of untagged HBx (2.3-fold) purified and refolded from inclusion bodies, suggesting that the soluble purified MBP−HBx protein retained much of its biological activity compared to refolded HBx (Figure S4A of the Supporting Information). To eliminate the possibility of the MBP tag interfering with the functionality of HBx, we tested the kinasing potential of the MBP−HBx protein after cleaving it with TEV protease. We observed that the phosphorylation potential of the Cdk2/cyclin E complex did not change even upon prolonged digestion of the MBP−HBx protein with TEV protease (Figure S4B of the Supporting Information).

The observations described above for HBx mutants X143 and X148 were reconfirmed using immunoprecipitates of the Cdk2/cyclin E complex from cells transfected individually with these recombinants along with previously described HBx recombinants X0−X4, X14, and X15.[11] The phosphorylation potential of wild-type HBx (X0) was nearly ∼2.3-fold higher than that of the vector control (Figure S5 of the Supporting Information). The cysteine mutants X143 and X148 showed moderate 1.7- and 1.3-fold increases in kinase activity, respectively, whereas mutants X3 and X4 did not support Cdk2 activity. These results strongly suggested that the cysteine residues in HBx are critical for its biological activity. Interestingly, the kinasing potential of other HBx mutants (X1, X2, X14, and X15) was close to the wild-type activity. Thus, the ability of these mutants to stimulate the Cdk2/cyclin E complex activity apparently correlated with their transactivation properties.[11]

Because the oncogenic potential of HBx is intimately linked to its transactivator functions, we also evaluated the transactivation potential of new cysteine mutants X143 and X148 on a viral promoter (Rous sarcoma virus) and a cellular promoter (Jun). Wild-type HBx (X0) was able to stimulate RSV and Jun promoters by 46- and 16-fold, respectively (Figure 1E,F), whereas X143 and X148 mutants showed lowered transactivator potential on both RSV (21- and 17-fold, respectively) and Jun promoters (11- and 9-fold, respectively). Thus, the loss of transactivation activity in X143 and X148 mutants combined with compromised cdk2/cyclin E kinase activity undeniably assigns a functional relevance to these cysteines in the structure of the HBx protein.

Determination of Disulfide Bonds in HBx by Mass Spectrometry. To realize maximal sequence coverage in MALDI-TOF/TOF analysis and assign disulfide bonds in HBx, the purified MBP−X0 fusion protein was subjected to proteolytic cleavage by two different proteases, trypsin and chymotrypsin. The MBP−X0 fusion protein exhibited a mass of 59.1 kDa corresponding to the combined mass of MBP (393 amino acids, 42.5 kDa) and HBx (154 amino acids, 16.5 kDa) (Figure S6 of the Supporting Information). The peptide mass fingerprint (PMF) pattern of the digested MBP−X0 fusion protein under reducing and nonreducing conditions revealed that a majority of the observed peptide ions $(M + H)^+$ were from HBx whereas the MBP peptides accounted for only a minor fraction (Table S1 of the Supporting Information). In addition, the exponentially modified protein abundance index (emPAI) values[34] from the nano LC−MS/MS analysis of selected samples supported the observations described above (Table S2 of the Supporting Information). Comparative analysis of the PMF patterns of HBx under reducing and nonreducing conditions showed the presence of distinguishing peptide ions $(M + H)^+$ containing either carbamidomethylated and disulfide-linked cysteines, respectively (Figure S7 of the Supporting Information). Annotated tandem mass spectra (MS/MS) corresponding to peptide sequences containing carbamidomethylated cysteine (reduced) are provided in Figure S8A−H of the Supporting Information along with their scores (Table S3 of the Supporting Information). We clearly observed five unique peptide ions showing the disulfide-linked status of six cysteines present in HBx (Table 1). Because of the increased accessibility of peptides to trypsin and chymotrypsin under reducing conditions, we observed shorter cysteine-containing peptides in the presence of DTT. The cysteine-containing peptides were observed in a disulfide-linked state under nonreducing conditions, whereas under reducing conditions, the peptides were detected at m/z values corresponding to their reduced and carbamidomethylated state.

Cys[7] Is Linked to Cys[69]. A peptide ion at m/z 1531.895 corresponding to peptide YC[7]QL linked to peptide SSAGPC[69]ALRF was detected for the chymotrypsin-digested MBP−X0

protein only under nonreducing conditions, but in the presence of DTT, the peptide ion was not observed (Figure 2A). Thus, these data provide evidence of the presence of a disulfide linkage between Cys[7] and Cys[69] of HBx protein.

Cys[61] Is Linked to Cys[115]. Another peptide ion at *m/z* 1617.854 was detected for the chymotrypsin-digested MBP−X0 protein in the absence of DTT (Figure 2B). Importantly, this ion was absent from the samples processed in the presence of DTT. The peptide ion mass corresponded with peptide RGLPVC[61]AF linked to peptide FKDC[115]VF. This result revealed the presence of another disulfide bond between Cys[61] and Cys[115].

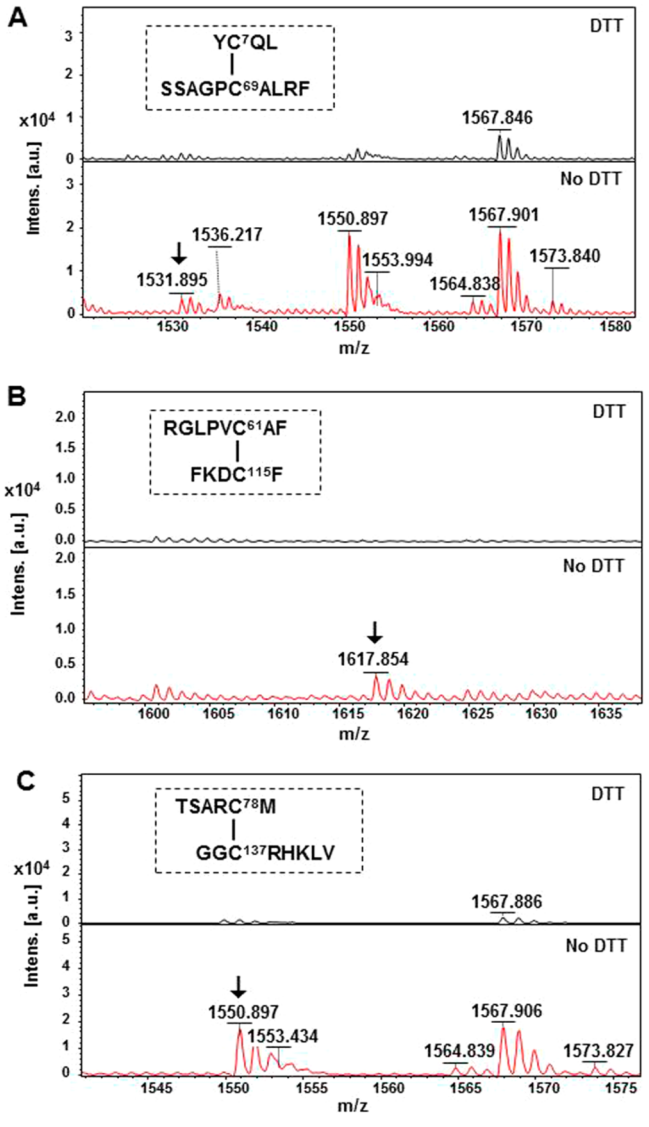

Figure 2. MALDI-TOF/TOF mass spectrometry analysis of disulfide-linked peptides from the MBP−X0 protein. The MBP−HBx protein was proteolytically cleaved with chymotrypsin overnight and subjected to mass spectrometry under reducing (DTT) or nonreducing (no DTT) conditions. (A) Peak at *m/z* 1531.895 (arrow) corresponding to disulfide-linked peptide YCQL-SSAGPCALRF containing Cys[7] and Cys[69] observed under nonreduced conditions and absent from the spectra obtained from reducing conditions. (B) Peak at *m/z* 1617.854 (arrow) corresponding to disulfide-linked peptide RGLPVCAF-FKDCF containing Cys[61] and Cys[115] observed under nonreducing conditions and absent from the spectra obtained from reducing conditions. (C) Peak at *m/z* 1550.897 (arrow) corresponding to disulfide-linked peptide TSARCM-GGCRHKLV containing Cys[78] and Cys[137] observed under nonreducing conditions and absent from the spectra obtained from reducing conditions.

Cys[78] Is Linked to Cys[137]. In the spectrum of the trypsin-digested MBP−X0 protein, we identified a peptide ion at *m/z* 3628.639 corresponding to peptide FTSARC[78]METTVDAHQILPKVLHK linked to VFVLGGC[137]R (Figure S9 of the Supporting Information). This peak was observed under only nonreducing conditions and was not detected under reducing conditions. Also, after an overnight digestion of the MBP−X0 fusion protein by chymotrypsin, we observed a peptide ion at *m/z* 1550.897 corresponding to peptide TSARC[78] M linked to GGC[137]RHKLV under nonreducing conditions but not under reducing conditions (Figure 2C), providing evidence of a disulfide linkage between Cys[78] and Cys[137] of the HBx protein.

Cys[17] Is Linked to Cys[143]. A peptide ion at *m/z* 1764.9 was detected under nonreducing conditions for the chymotrypsin-digested and alkylated MBP−X0 samples but missing from the corresponding reduced samples (Figure 3A). This ion corresponded to peptide C[17]L linked to C-terminal peptide VC[143]APAPC[148]NFF that had two cysteines. As both cysteines of the C-terminal peptide were oxidized, it led to ambiguity in identifying the correct cysteine that bridged the C[17]L peptide. To resolve the ambiguity in the final disulfide linkage, we sequenced the peptide ion at *m/z* 1764.9. The peptide was not readily amenable to fragmentation, and we observed residues V and R from peptide VPRLCL and residues A, F, and F from C-terminal peptide VCAPAPCNFF upon sequencing (Figure 3B). In the fragmented MS/MS spectra of the 1764.9 Da peptide ion, we observed a peak at *m/z* 566.44 that corresponded to peptide LC[17]L linked to VC[143]. Therefore, the fourth disulfide linkage was assigned between Cys[17] and Cys[143]. The C-terminal cysteine was shown to be free.

Cys[148] Bonds with Cys[17] in the Absence of Cys[143]. As both Cys[143] and Cys[148] were observed in the oxidized state, we investigated the disulfide bonding pattern in the MBP−X143 and MBP−X148 mutants. The MALDI-TOF/TOF-based comparative analysis of the tryptic and chymotryptic fragments of MBP−X143 and MBP−X148 fusion proteins under native and reducing conditions confirmed the presence of a peptide ion at *m/z* 1284.6 corresponding to the disulfide-linked status of Cys[17] and Cys[148] in the MBP−X143 protein and Cys[17] and Cys[143] in the MBP−X148 protein, respectively (Figure S10 of the Supporting Information). The disulfide bonding pattern of the remaining cysteines remained unchanged in the two mutant proteins (data not shown). In the absence of Cys[143], Cys[148] is able to participate in the formation of a disulfide linkage with Cys[17] by virtue of being closely spaced to Cys[143] and possessing spatial freedom to interact with Cys[17].

In addition, the emPAI-based analysis from nano LC−MS/MS data (Table S2 of the Supporting Information) and sequence coverage showed relatively fewer HBx-derived peptide sequences that were reproducibly observed and identified in the MBP−X148 mutant, while in the MBP−X143 mutant, the ratio was comparable between HBx- and MBP-derived peptides. We also used the neural network and web-based server DiANNA that is commonly used for predicting disulfide bonds in proteins.[28]

Interestingly, our findings on disulfide bridges in HBx revealed a much stronger (50%) similarity to that predicted by DiANNA, making this study more plausible than any previous report (Table 2). The four disulfide linkages in a biologically active HBx are illustrated in Figure 4.

dx.doi.org/10.1021/bi500140t | *Biochemistry* 2014, 53, 4685−4695

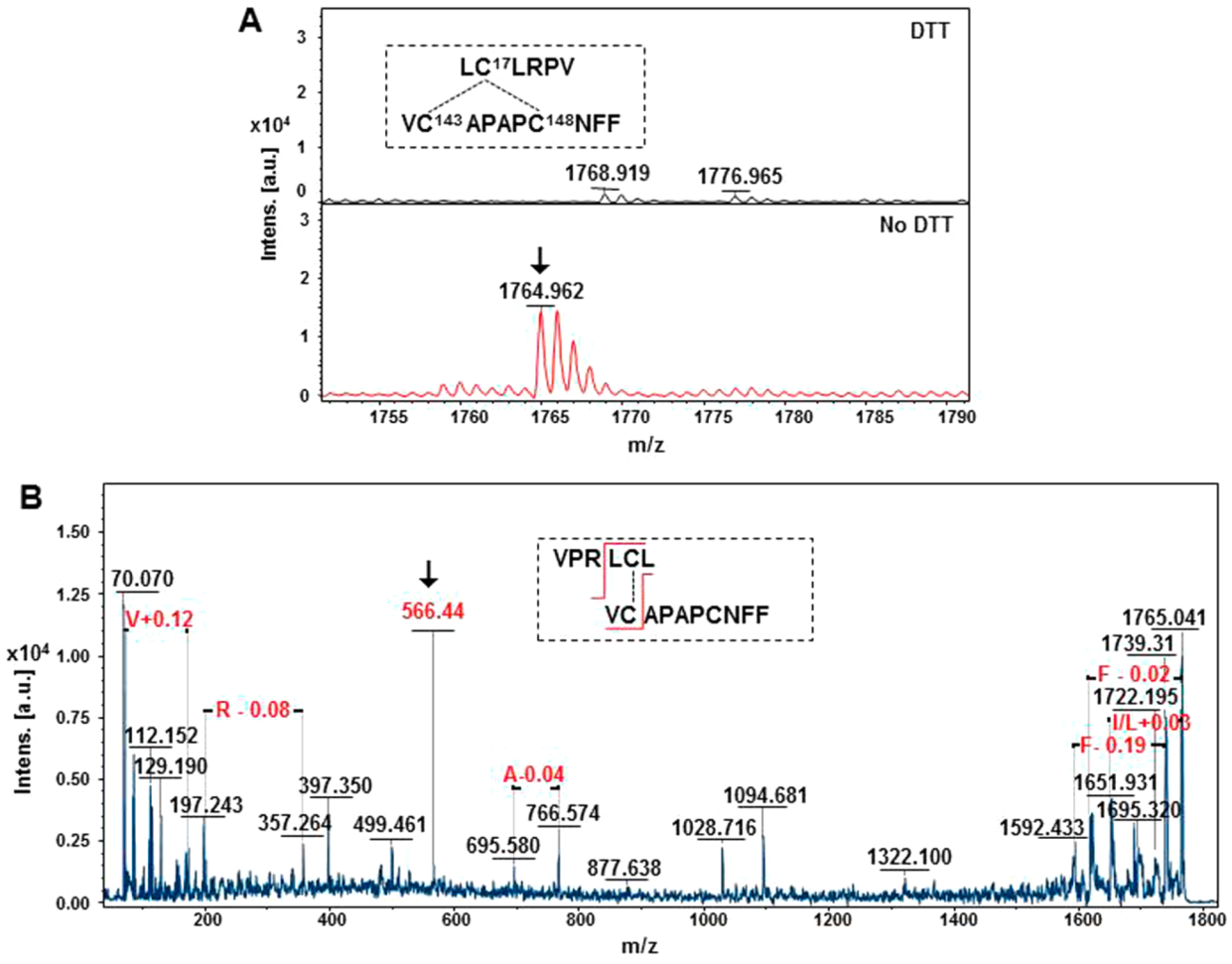

Figure 3. MALDI-TOF/TOF mass spectrometry analysis of disulfide-linked peptide LCLRPV-VCAPAPCNFF. The MBP−X0 protein was proteolytically cleaved with chymotrypsin and subjected to mass spectrometry under reducing (DTT) or nonreducing (no DTT) conditions. (A) Peak at m/z 1764.962 (arrow) corresponding to a disulfide-linked peptide containing Cys^{17}, Cys^{143}, and Cys^{148} observed under nonreducing conditions and absent from the spectra obtained from reducing conditions. (B) Tandem mass spectrum of the precursor ion at m/z 1764.962. The ion at m/z 566.44 (arrow) corresponds to disulfide-linked peptide ion LCL-VC containing Cys^{17} and Cys^{143}.

Table 2. Disulfide Linkages in the HBx Protein As Predicted by DiANNA and Experimentally Determined in This Study

	prediction by DiANNA	determined of MS (this study)
linked	C7−C69	C7−C69
linked	C17−C61	C17−C143
linked	C115−C148	C61−C115
linked	C78−C137	C78−C137
free	C143	C148

DISCUSSION

Cysteine residues in proteins are well-known to stabilize the structure of proteins, conduct catalytic activity, acquire cofactor binding properties, and facilitate intermolecular interactions, and their loss or mutation results in misfolding of proteins, loss of activity, and mislocalization in the cell.[35−38] Disulfide bonds play a significant role in determining and stabilizing the tertiary and quaternary structure of a protein.[39] Disulfide bonds are mostly reported in proteins destined for mitochondria, extracellular secretion, and prokaryotic periplasm. However, pathways leading to the formation of disulfide bonds in cytoplasmic proteins that are important for the biogenesis of some viruses have been elucidated.[40]

One of the major impediments in determining the molecular structure of HBx is its intrinsically disordered structure that causes it to be routed to inclusion bodies upon overexpression in bacterial systems. Intrinsic disorder provides the protein with several functional advantages, including an increased surface area for interaction, flexibility to interact with structurally diverse molecules (proteins, nucleic acids, and metal ions), the ability to undergo ligand-induced disorder−order transition, efficient regulation through accessible post-translational modification, and accessible proteolytic cleavage sites.[41] Disordered proteins are frequently implicated in cancer, cardiovascular diseases, and neurodegenerative diseases.[42] Despite bestowing obvious functional advantages upon proteins, intrinsic disorder greatly hinders the determination of the structure of proteins.

Most of the structural characterization studies of HBx to date have been conducted using refolded protein purified from *E. coli*-derived inclusion bodies without providing any supporting evidence of their biological activity. In this study, HBx protein was purified as a soluble protein with the aid of the maltose binding protein tag in the SHuffle strain of *E. coli*, which has been engineered to facilitate disulfide bond formation and correct protein folding.[27] The purified MBP−HBx fusion protein was found to be biologically active as it was able to enhance the potential of Cdk2/cyclin E to phosphorylate its substrate histone

dx.doi.org/10.1021/bi500140t | *Biochemistry* 2014, 53, 4685−4695

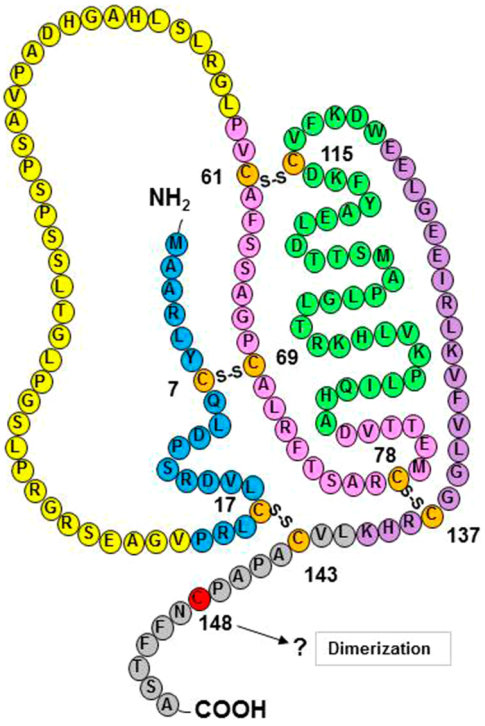

Figure 4. Schematic representation of the disulfide linkages in HBx. The primary sequence of HBx (154 amino acids) is shown as a chain of beads representing individual amino acids. The six conserved domains of HBx are colored blue (A), yellow (B), pink (C), green (D), purple (E), and gray (F). The eight disulfide-linked (S–S) cysteines (C^{7}–C^{69}, C^{17}–C^{143}, C^{61}–C^{115}, and C^{78}–C^{137}) as determined mass spectrometry in this study are colored orange. The only free cysteine (C^{148}) is colored red.

H1. The ability of the cysteine mutants of HBx either to potentiate the Cdk2/cyclin E kinase activity or to transactivate promoter reporter genes has been compromised. These results imply that the cysteine residues of HBx are functionally relevant at least in the present context as opposed to some earlier reports.[43]

Five of the nine conserved cysteines of HBx have been functionally characterized through site-directed mutagenesis. In two separate studies, Cys^{61}, Cys^{69}, and Cys^{137} mutations have been shown to abrogate the transactivation potential of HBx on multiple cellular and viral promoters.[11] In addition, Cys^{61} and Cys^{69} mutations are also associated with weakened binding of HBx to UVDDB, through which it is known to inhibit the DNA repair pathway.[21] Recently, a C-terminal region of HBx was reported to be essential for its mitochondrial targeting, where Cys^{115} was found to be a critical residue.[19] Mutation of Cys^{7} apparently does not affect the transcriptional activation property of HBx because it lies in its N-terminal transrepression domain.[44] The deletion of 20 C-terminal amino acids of HBx (F domain) leading to a reduced half-life of the protein, poor transactivation, and impaired HBV replication[45] could be due to the deletion of three cysteine residues (viz., C^{137}, C^{143}, and C^{148}) and disruption of disulfide linkages. Note that X15 (ΔA, B, and F domain) is very unstable compared to X0 in mammalian cells. Thus, disulfide linkages may be critical for the intracellular stability and biological activity of HBx. All these reports nevertheless suggest the importance of different cysteines in HBx conducting various functions.

The MBP–X0 fusion protein showed an apparent molecular mass of ~60 kDa in an SDS–PAGE gel and a mass of 59.182 kDa obtained via MALDI-TOF mass spectrometry. These masses correspond to the MBP–X0 processed fusion protein where the MBP signal sequence of 26 amino acid residues is cleaved off during its transport into the periplasm of *E. coli*.[46] Thus, our findings suggest that a major fraction of the MBP–HBx fusion protein is transported into the periplasm, where the process of disulfide bond formation is catalyzed. Briefly, proteins with the signal sequence remain unfolded after translation in the cytoplasm and are transported via the Sec pathway into the periplasm[47] where disulfide oxidoreductase DsbA catalyzes disulfide bonds vectorially (from N- to C-terminus).[48] These linkages are further corrected to the native state by disulfide isomerase DsbC. Note that in previous studies the disulfide linkages in HBx were established using refolded recombinant protein preparations that may have the disadvantage of acquiring both native and non-native disulfide bonds during the unfolding–refolding exercise.[16,23,24] In addition, no evidence of the biological activity of these preparations was provided.

In addition to determining the tertiary and quaternary structure of proteins, disulfide bonds form a part of the active site in proteins, allosterically regulate protein function, and stabilize protein structure.[49] Using mass spectrometry, we could unambiguously assign four disulfide linkages in the HBx protein. The patterns of disulfide bonds from the peptide mass fingerprint obtained using two separate enzymes, trypsin and chymotrypsin, were similar, suggesting that the results were reproducible under different proteolytic digestion conditions. Further, the exponentially modified protein abundance index (emPAI), a scale for measuring the relative abundance of proteins in a sample based on protein coverage by the peptide matches from a database search,[34] revealed that the relative abundance of peptides from HBx (emPAI of 16.0) was much higher than that from its fusion partner, MBP (emPAI of 11.5), despite its much larger size (Table S2 of the Supporting Information). A higher emPAI value suggests that HBx is more easily accessible to the proteolytic enzymes than its fusion partner, MBP.

The disulfide bonds identified distinctly in the MBP–X0 fusion protein were between Cys^{7} and Cys^{69}, Cys^{61} and Cys^{115}, Cys^{78} and Cys^{137}, and Cys^{17} and Cys^{143} (Table 2), while Cys148 was observed to be free. Interestingly, mass spectrometric analysis of disulfides in MBP fusion HBx mutants (MBP–X143 and MBP–X148) exhibited a disulfide link between Cys^{148} and Cys^{17} in the context of Cys^{143} being mutated. This may be a consequence of disulfide shuffling, which tends to occur in peptides when a free cysteine is present in the proximity of a disulfide bond.[50] In the absence of the primary disulfide partner, the other closely spaced cysteine may form a permanent disulfide bond. Such disulfide shuffling may be functionally relevant as in the case of Sindbis and Semliki forest virus that allows contact with plasma membrane for viral entry.[51]

Previously, we and others have shown that HBx can also form homodimers and that such dimerization is sensitive to reducing agents.[15,17] In concordance, we also observed disulfide-based oligomerization of HBx protein by differential mobility of the HBx band in reducing and nonreducing SDS–PAGE gels (Figure S11A,B of the Supporting Information). We wondered if the cysteine mutants of HBx will migrate differentially under reducing and nonreducing experimental conditions. Therefore, we analyzed the electrophoretic mobility of affinity-purified MBP–HBx recombinant protein and its two cysteine mutants, MBP–X143 and MBP–X148. As shown in Figure S11D of the Supporting Information, the intensity of the dimeric form of the MBP–X148 protein was much lower than those of the dimeric

dx.doi.org/10.1021/bi500140t | *Biochemistry* 2014, 53, 4685–4695

forms of the MBP−HBx or MBP−X143 mutant, suggesting that mutation of cysteine 148 in HBx adversely affected its dimerization function. Our observation for HBx is supported by a previous report on the 16 kDa protein of infectious bronchitis virus (IBV), which showed the involvement of multiple cysteines in the dimerization process. The IBV 16 kDa protein showed varying degrees of dimerization and oligomerization when individual cysteines were mutated, and a complete loss of the dimer form was observed only when all 11 conserved cysteines were mutated.[52] Thus, a marked reduction in the level of the dimeric form of the MBP−X148 protein suggests that Cys^{148} seems to be involved in the dimerization and oligomerization function of HBx. This conjecture is further strengthened by reports that other viral oncoproteins, resembling many transcription factors, conduct transactivation functions via protein−protein interactions.[53] For example, HTLV Tax1 protein carries a cysteine- and histidine-rich zinc finger domain, which is essential for its homodimerization.[54] Likewise, the heterodimerization of Tax1 is critical for CREB and NF-κB transactivation,[55] while HIV Tat protein contains a cysteine-rich region that promotes metal-mediated dimer formation.[56] Mutation of cysteine residues in Tat severely impacts its transactivation potential.[57] The E6 protein of human papilloma virus is a 150-amino acid cysteine-rich protein that self-associates through its N-terminal zinc binding domain.[58] More recently, the solution structure of the N-terminal domain of the E6 protein was reported; the cysteines at the dimer interface were mutated to increase the solubility of protein because dimerization made the protein less amenable to structural studies.[59]

Our future endeavors will be to determine the solution structure of HBx as a MBP fusion protein or after cleavage from the MBP fusion. The determination of the HBx structure will shed additional light on its pleiotropic effects in various cellular functions. The participation of HBx in the development of HCC in chronic HBV cases makes it an attractive candidate for the development of antiviral therapeutics.

■ ASSOCIATED CONTENT

Supporting Information

CD spectra of MBP, MBP−HBx, MBP−X143, and MBP−X148 proteins; parameters for identification of the HBx protein in different samples from PMF patterns, including database, sequence coverage, modifications, missed cleavages, MOWSE scores, etc.; emPAI index values calculated for HBx and MBP domains in MBP−X0, MBP−X143, and MBP−X148 proteins from nano LC−MS/MS data; schematic representation of the workflow followed for MALDI-TOF/TOF mass spectrometry to identify disulfide bonds in the HBx protein; purification of the MBP−X0 protein and cytoplasmic and periplasmic fractionation of MBP−X0 protein-harboring *E. coli* cells; *in vitro* phosphorylation assay of HBx cysteine mutants; intact mass spectra of the MBP−X0 protein; nano LC−MS/MS-based sequencing of cysteine-containing peptides in trypsin- or chymotrypsin-digested MBP−X0 protein along with the score for each MS/MS spectrum; MALDI-TOF/TOF analysis of disulfide linkages of C-terminal cysteines of MBP−X143 and MBP−X148 proteins; and SDS−PAGE showing oligomerization of HBx under nonreducing conditions. This material is available free of charge via the Internet at http://pubs.acs.org.

■ AUTHOR INFORMATION

Corresponding Author

*Virology Group, International Centre for Genetic Engineering and Biotechnology, Aruna Asaf Ali Marg, New Delhi 110067, India. Telephone: +91-11-26741680. Fax: +91-11-26742316. E-mail: vijay@icgeb.res.in.

Funding

This work was supported in part by a J. C. Bose National Fellowship (Grant SR/S2/JCB-80/2012) from the Department of Science and Technology, Government of India, New Delhi (to V.K.). K.S. has been the recipient of a senior research fellowship of the Council of Scientific and Industrial Research, New Delhi.

Notes

The authors declare no competing financial interest.

■ ACKNOWLEDGMENTS

We are grateful to Dr. Dinkar Sahal for critical reading of the manuscript. We also thank Dr. A. Weisz (University of Napoli, Naples, Italy) for the JUN_CAT reporter construct and Dr. J. A. Wolff (University of Wisconsin, Madison, WI) for the RSV_CAT reporter construct.

■ ABBREVIATIONS

CAT, chloramphenicol acetyltransferase; HBx, hepatitis B virus X protein; MALDI, matrix-assisted laser desorption and ionization; MBP, maltose binding protein; MS, mass spectrometry; TOF, time-of-flight.

■ REFERENCES

(1) Iakoucheva, L. M., Brown, C. J., Lawson, J. D., Obradović, Z., and Dunker, A. K. (2002) Intrinsic disorder in cell-signaling and cancer-associated proteins. *J. Mol. Biol. 323*, 573−584.

(2) Benhenda, S., Cougot, D., Buendia, M. A., and Neuveut, C. (2009) Hepatitis B virus X protein molecular functions and its role in virus life cycle and pathogenesis. *Adv. Cancer Res. 103*, 75−109.

(3) Tian, Y., Yang, W., Song, J., Wu, Y., and Ni, B. (2013) Hepatitis B virus X protein-induced aberrant epigenetic modifications contributing to human hepatocellular carcinoma pathogenesis. *Mol. Cell. Biol. 33*, 2810−2816.

(4) Kumar, V., and Sarkar, D. P. (2004) Hepatitis B Virus X protein (HBx): Structure-function relationships and role in viral pathogenesis. In *Handbook of Experimental Pharmacology* (Triezenberg, S. J., Kaufman, J., and Gossen, M., Eds.) pp 377−407, Springer-Verlag, Duesseldorf, Germany.

(5) Bouchard, M., and Schneider, R. J. (2005) The enigmatic X gene of hepatitis B virus. *J. Virol. 78*, 12725−12734.

(6) Benn, J., and Schneider, R. J. (1995) Hepatitis B virus HBx protein deregulates cell cycle checkpoint controls. *Proc. Natl. Acad. Sci. U.S.A. 92*, 11215−11219.

(7) Mukherji, A., Janbandhu, V. C., and Kumar, V. (2007) HBx-dependent cell cycle deregulation involves interaction with cyclin E/A-cdk2 complex and destabilization of p27Kip1. *Biochem. J. 401*, 247−256.

(8) Nijhara, R., Jana, S. S., Goswami, S. K., Rana, A., Majumdar, S. S., Kumar, V., and Sarkar, D. P. (2001) Sustained activation of mitogen-activated protein kinases and activator protein 1 by the hepatitis B virus X protein in mouse hepatocytes in vivo. *J. Virol. 75*, 10348−10358.

(9) Klein, N. P., and Schneider, R. J. (1997) Activation of Src family kinases by hepatitis B virus HBx protein and coupled signaling to Ras. *Mol. Cell. Biol. 17*, 6427−6436.

(10) Bouchard, M. J., Wang, L. H., and Schneider, R. J. (2001) Calcium signaling by HBx protein in hepatitis B virus DNA replication. *Science 294*, 2376−2378.

(11) Kumar, V., Jayasuryan, N., and Kumar, R. (1996) A truncated mutant (residues 58−140) of the hepatitis B virus X protein retains transactivation function. *Proc. Natl. Acad. Sci. U.S.A. 93*, 5647−5652.

(12) Reddi, H., Kumar, R., Jain, S. K., and Kumar, V. (2003) A carboxy-terminal region of the hepatitis B virus X protein promotes DNA interaction of CREB and mimics the native protein for transactivation function. *Virus Genes 26*, 227−238.
(13) Misra, K. P., Mukherji, A., and Kumar, V. (2004) The conserved amino-terminal region (amino acids 1−20) of the hepatitis B virus X protein shows a transrepression function. *Virus Res. 105*, 157−165.
(14) Nijhara, R., Jana, S. S., Goswami, S. K., Kumar, V., and Sarkar, D. P. (2001) An internal segment (residues 58−119) of the hepatitis B virus X protein is sufficient to activate MAP kinase pathways in mouse liver. *FEBS Lett. 504*, 59−64.
(15) Reddi, H. V., and Kumar, V. (2004) Self-association of the hepatitis B virus X protein in the yeast two-hybrid system. *Biochem. Biophys. Res. Commun. 317*, 1017−1022.
(16) Urban, S., Hildt, E., Eckerskorn, C., Sirma, H., Kekulé, A., and Hofschneider, P. H. (1997) Isolation and molecular characterization of hepatitis B virus X-protein from a baculovirus expression system. *Hepatology 26*, 1045−1053.
(17) Lin, M. H., and Lo, S. C. (1989) Dimerization of hepatitis B viral X protein synthesized in a cell-free system. *Biochem. Biophys. Res. Commun. 164*, 14−21.
(18) Kidd-Ljunggren, K., Oberg, M., and Kidd, A. H. (1995) The hepatitis B virus X gene: Analysis of functional domain variation and gene phylogeny using multiple sequences. *J. Gen. Virol. 76*, 2119−2130.
(19) Li, S. K., Ho, S. F., Tsui, K. W., Fung, K. P., and Waye, M. Y. (2008) Identification of functionally important amino acid residues in the mitochondria targeting sequence of hepatitis B virus X protein. *Virology 381*, 81−88.
(20) Waris, G., Huh, K. W., and Siddiqui, A. (2001) Mitochondrially associated hepatitis B virus X protein constitutively activates transcription factors STAT-3 and NF-κB via oxidative stress. *Mol. Cell. Biol. 21*, 7721−7730.
(21) Becker, S. A., Lee, T. H., Butel, J. S., and Slagle, B. L. (1998) Hepatitis B virus X protein interferes with cellular DNA repair. *J. Virol. 72*, 266−272.
(22) Rui, E., Moura, P. R., Gonçalves, K. A., Rooney, R. J., and Kobarg, J. (2006) Interaction of the hepatitis B virus protein HBx with the human transcription regulatory protein p120E4F in vitro. *Virus Res. 115*, 31−42.
(23) Gupta, A., Mal, T. K., Jayasuryan, N., and Chauhan, V. S. (1995) Assignment of disulphide bonds in the X protein (HBx) of hepatitis B virus. *Biochem. Biophys. Res. Commun. 212*, 919−924.
(24) Marczinovits, I., Molnár, J., Kele, M. Z., Szabó, P. T., and Janáky, T. (1998) A simple folding method for high level production of the hydrophobic disulfide bonded hepatitis B X protein by inclusion body route and its structural analysis. In *Stability and Stabilization of Biocatalysts (Progress in Biotechnology)* (Ballesteros, A., Plou, F. J., Iborra, J. L., and Halling, P. J., Eds.) pp 296−274, Elsevier Science BV, Amsterdam.
(25) Haviv, I., Vaizel, D., and Shaul, Y. (1996) pX, the HBV-encoded coactivator, interacts with components of the transcription machinery and stimulates transcription in a TAF-independent manner. *EMBO J. 15*, 3413−3420.
(26) Kalra, N., and Kumar, V. (2004) c-Fos is a mediator of the c-myc-induced apoptotic signaling in serum-deprived hepatoma cells via the p38 mitogen-activated protein kinase pathway. *J. Biol. Chem. 279*, 25313−25319.
(27) Lobstein, J., Emrich, C. A., Jeans, C., Faulkner, M., Riggs, P., and Berkmen, M. (2012) SHuffle, a novel *Escherichia coli* protein expression strain capable of correctly folding disulfide bonded proteins in its cytoplasm. *Microb. Cell Fact. 11*, 56−72.
(28) Park, C., and Raines, R. T. (2001) Adjacent cysteine residues as a redox switch. *Protein Eng. 14*, 939−942.
(29) de-Medina, T., Haviv, I., Noiman, S., and Shaul, Y. (1994) The X protein of hepatitis B virus has a ribo/deoxy ATPase activity. *Virology 202*, 401−407.
(30) Ferrè, F., and Clote, P. (2006) DiANNA 1.1: An extension of the DiANNA web server for ternary cysteine classification. *Nucleic Acids Res. 34*, W182−W185.
(31) Raran-Kurussi, S., and Waugh, D. S. (2012) The ability to enhance the solubility of its fusion partners is an intrinsic property of maltose-binding protein but their folding is either spontaneous or chaperone-mediated. *PLoS One 7*, e49589.
(32) Sato, Y., and Inaba, K. (2012) Disulfide bond formation network in the three biological kingdoms, bacteria, fungi and mammals. *FEBS J. 279*, 2262−2271.
(33) Quiocho, F. A., Spurlino, J. C., and Rodseth, L. E. (1997) Extensive features of tight oligosaccharide binding revealed in high-resolution structures of the maltodextrin transport/chemosensory receptor. *Structure 5*, 997−1015.
(34) Ishihama, Y., Oda, Y., Tabata, T., Sato, T., Nagasu, T., Rappsilber, J., and Mann, M. (2005) Exponentially modified protein abundance index (emPAI) for estimation of absolute protein amount in proteomics by the number of sequenced peptides per protein. *Mol. Cell. Proteomics 4*, 1265−1272.
(35) Fomenko, D. E., Marino, S. M., and Gladyshev, V. N. (2008) Functional diversity of cysteine residues in proteins and unique features of catalytic redox-active cysteines in thiol oxidoreductases. *Mol. Cells 26*, 228−235.
(36) Gu, W. J., Corti, O., Araujo, F., Hampe, C., Jacquier, S., Lücking, C. B., Abbas, N., Duyckaerts, C., Rooney, T., Pradier, L., Ruberg, M., and Brice, A. (2003) The C289G and C418R missense mutations cause rapid sequestration of human Parkin into insoluble aggregates. *Neurobiol. Dis. 14*, 357−364.
(37) Kiritsi, M. N., Fragoulis, E. G., and Sideris, D. C. (2012) Essential cysteine residues for human RNase κ catalytic activity. *FEBS J. 279*, 1318−1326.
(38) Nazareth, L. V., Stenoien, D. L., Bingman, W. E., III, James, A. J., Wu, C., Zhang, Y., Edwards, D. P., Mancini, M., Marcelli, M., Lamb, D. J., and Weigel, N. L. (1999) A C619Y mutation in the human androgen receptor causes inactivation and mislocalization of the receptor with concomitant sequestration of SRC-1 (steroid receptor coactivator 1). *Mol. Endocrinol. 13*, 2065−2075.
(39) Krey, T., d'Alayer, J., Kikuti, C. M., Saulnier, A., Damier-Piolle, L., Petitpas, I., Johansson, D. X., Tawar, R. G., Baron, B., Robert, B., England, P., Persson, M. A., Martin, A., and Rey, F. A. (2010) The disulfide bonds in glycoprotein E2 of hepatitis C virus reveal the tertiary organization of the molecule. *PLoS Pathog. 6*, e1000762.
(40) Saaranen, M. J., and Ruddock, L. W. (2013) Disulfide bond formation in the cytoplasm. *Antioxid. Redox Signaling 19*, 46−53.
(41) Cortese, M. S., Uversky, V. N., and Dunker, A. K. (2008) Intrinsic disorder in scaffold proteins: Getting more from less. *Prog. Biophys. Mol. Biol. 98*, 85−106.
(42) Uversky, V. N., and Dunker, A. K. (2010) Understanding protein non-folding. *Biochim. Biophys. Acta 1804*, 1231−1264.
(43) de Moura, P. R., Rui, E., de Almeida Gonçalves, K., and Kobarg, J. (2005) The cysteine residues of the hepatitis B virus onco-protein HBx are not required for its interaction with RNA or with human p53. *Virus Res. 108*, 121−131.
(44) Murakami, S., Cheong, J. H., and Kaneko, S. (1994) Human hepatitis virus X gene encodes a regulatory domain that represses transactivation of X protein. *J. Biol. Chem. 269*, 15118−15123.
(45) Lizzano, R. A., Yang, B., Clippinger, A. J., and Bouchard, M. J. (2011) The C-terminal region of the hepatitis B virus X protein is essential for its stability and function. *Virus Res. 155*, 231−239.
(46) Puziss, J. W., Harvey, R. J., and Bassford, P. J., Jr. (1992) Alterations in the hydrophilic segment of the maltose-binding protein (MBP) signal peptide that affect either export or translation of MBP. *J. Bacteriol. 174*, 6488−6497.
(47) Baneyx, F., and Mujacic, M. (2004) Recombinant protein folding and misfolding in *Escherichia coli*. *Nat. Biotechnol. 22*, 1399−1408.
(48) Depuydt, M., Messens, J., and Collet, J. F. (2011) How proteins form disulfide bonds. *Antioxid. Redox Signaling 15*, 49−66.
(49) Zhang, L., Chou, C. P., and Moo-Young, M. (2011) Disulfide bond formation and its impact on the biological activity and stability of recombinant therapeutic proteins produced by *Escherichia coli* expression system. *Biotechnol. Adv. 29*, 923−929.

(50) Yen, T. Y., Yan, H., and Macher, B. A. (2002) Characterizing closely spaced, complex disulfide bond patterns in peptides and proteins by liquid chromatography/electrospray ionization tandem mass spectrometry. *J. Mass Spectrom. 37*, 15−30.
(51) Glomb-Reinmund, S., and Kielian, M. (1998) The role of low pH and disulfide shuffling in the entry and fusion of Semliki Forest virus and Sindbis virus. *Virology 248*, 372−381.
(52) Ng, L. F., and Liu, D. X. (2002) Membrane association and dimerization of a cysteine-rich, 16-kilodalton polypeptide released from the C-terminal region of the coronavirus infectious bronchitis virus 1a polyprotein. *J. Virol. 76*, 6257−6267.
(53) Amoutzias, G. D., Robertson, D. L., Van de Peer, Y., and Oliver, S. G. (2008) Choose your partners: Dimerization in eukaryotic transcription factors. *Trends Biochem. Sci. 33*, 220−229.
(54) Semmes, O. J., and Jeang, K. T. (1992) HTLV-I Tax is a zinc-binding protein: Role of zinc in Tax structure and function. *Virology 188*, 754−764.
(55) Tie, F., Adya, N., Greene, W. C., and Giam, C. Z. (1996) Interaction of the human T-lymphotropic virus type 1 Tax dimer with CREB and the viral 21-base-pair repeat. *J. Virol. 70*, 8368−8374.
(56) Frankel, A. D., Bredt, D. S., and Pabo, C. O. (1988) Tat protein from human immunodeficiency virus forms a metal-linked dimer. *Science 240*, 70−73.
(57) Garcia, J. A., Harrich, D., Pearson, L., Mitsuyasu, R., and Gaynor, R. B. (1988) Functional domains required for tat-induced transcriptional activation of the HIV-1 long terminal repeat. *EMBO J. 7*, 3143−3147.
(58) Lipari, F., McGibbon, G. A., Wardrop, E., and Cordingley, M. G. (2001) Purification and biophysical characterization of a minimal functional domain and of an N-terminal Zn^{2+}-binding fragment from the human papillomavirus type 16 E6 protein. *Biochemistry 40*, 1196−1204.
(59) Zanier, K., M'hamed ould Sidi, A., Boulade-Ladame, C., Rybin, V., Chappelle, A., Atkinson, A., Kieffer, B., and Travé, G. (2012) Solution structure analysis of the HPV16 E6 oncoprotein reveals a self-association mechanism required for E6-mediated degradation of p53. *Structure 20*, 604−617.